

ARTICLES

Complex Self-Assembly of Hyperbranched Polyamidoamine/Linear Polyacrylic Acid in Water and Their Functionalization

Yongwen Zhang, Wei Huang,* Yongfeng Zhou, and Deyuan Yan*

*School of Chemistry and Chemical Engineering, State Key Laboratory of Metal Matrix Composites, Shanghai Jiao Tong University, 800 Dongchuan Road, Shanghai, 200240, P.R. China**Received: November 20, 2008; Revised Manuscript Received: March 18, 2009*

This paper studied the complex self-assembly of hyperbranched polyamidoamine (h-PAMAM) and linear polyacrylic acid (l-PAA) by the facile mixing of their aqueous solutions. The complex self-assembly behavior and mechanism were investigated by the optical microscopy, UV–vis spectrometer, TEM, and ζ potential measurements. Interestingly, various self-assembled aggregates from micelles to microscaled vesicles were obtained by adjusting the solution pH. Moreover, the hollow structure of the vesicles was successfully stabilized by using glutaric dialdehyde (GDA) to cross-link the PAMAM layer. As expected, the resulting hollow spheres were able to capture different noble metal ions from their aqueous solution and reduce them into nanoparticles in situ, hence forming the hybrid hollow spheres. Such hybrid hollow spheres might have potential application in catalytic fields.

1. Introduction

In recent years, the self-assembly objects with nanostructures based on polymers have attracted increasing attention due to their wide applications in scientific and technical fields.¹ Among them, hollow spheres with various diameters (from nanometer to micrometer scale) have aroused especially great interests because they can be potentially used as the carriers of catalysts, enzymes, drugs, etc.² To date, several famous research groups (such as Eisenberg's,^{1d} Meijer's,¹ⁱ Armes',^{2a} Bates',^{2d} Rotello's,^{2e} and Jiang's^{1g} groups) have reported some novel self-assembly strategies and fabricated a lot of charming hollow spheres. For example, one kind of hollow sphere was studied most extensively on the basis of the micellization of block or graft copolymers in selective solvents.³ Another kind of hollow spheres was also prepared by using templates to form core–shell particles, subsequently removing the core.⁴ Besides, a peculiar class of hollow spheres were also fabricated effectively on the basis of some rigid-coil polymer pairs,^{5a} positively charged polymer pairs,^{5b} or complementary random copolymers possessing hydrogen bonding sites.^{5c,d} In these pioneering works, the self-assembly process was often driven by hydrophobic interactions, intermolecular hydrogen bonds, parallel packing of rigid chains, and so forth. Furthermore, some approaches based on cross-linking reaction were usually adopted to stabilize the self-assembled hollow spheres because this is very important to their applications.⁶

Hyperbranched polymers are a kind of highly branched macromolecule with three-dimensional architecture and numerous terminal groups, which can be synthesized conveniently in high yields. Such features have made them promising materials for supramolecular self-assembly.⁷ For example, some hollow spheres (giant vesicles) were successfully obtained by the self-

assembly of hyperbranched poly(3-ethyl-3-oxetanemethanol)-based polymers in recent work of our group.⁸ Here we describe a novel kind of hollow sphere by the complex self-assembly of hyperbranched polyamidoamine (h-PAMAM) and linear polyacrylic acid (l-PAA) in water. The self-assembly behavior and mechanism in water was exploited in detail and then the stabilization of hollow structures by the cross-linking technology to produce functional hollow spheres was also studied. We find that this assembly process is driven by the specific interactions between the amino subunits in the h-PAMAM and carboxyl groups in the l-PAA. Besides, various morphologies of the self-assembled aggregates can be realized by adjusting the solution pH. More importantly, the cross-linked hollow spheres can serve as the template and reductant to capture different noble metal ions, reduce them into nanoparticles in situ, and form hybrid hollow spheres. As a result, this type of hollow sphere can be potentially applied as the effective catalyst carriers.

2. Experimental Section

2.1. Materials. Polyacrylic acid (35 wt % solution in water, M_w 100 000; acid value 698 mg of KOH/g), *N,N'*-methylenebisacrylamide (MBA, 99%), 1-(2-aminoethyl)piperazine (AEPZ, 99%), and fluorescein isothiocyanate isomer I (FITC, 90%) were purchased from Aldrich. Silver nitrate (AgNO_3), chloroauric acid tetrahydrate ($\text{HAuCl}_4 \cdot 4\text{H}_2\text{O}$), palladium(II) chloride (PdCl_2), glutaric dialdehyde aqueous solution (GDA, 25 wt %), hydrochloric acid (HCl), and sodium hydroxide (NaOH) were purchased from Sino-pharm Chemical Reagent Co., Ltd.

2.2. Preparation of the Hyperbranched Polyamidoamine. The h-PAMAM with terminated amine groups was synthesized according to our previous work.⁹ Briefly, the Michael addition polymerization of MBA with AEPZ at equal feed molar ratio was carried out in water until the vinyl groups of MBA were

* E-mail: hw66@sjtu.edu.cn (Wei Huang), dyyan@sjtu.edu.cn (Deyuan Yan); Fax: (+86)-21-5474-1297; Tel: (+86)-21-5474-2665.

consumed away. The degree of branching (DB) = 0.42; $M_n = 26\ 000$; $M_w/M_n = 2.3$. The total amine value was 5200 mg of KOH/g.¹⁰

2.3. Preparation of Complex Self-Assembled Polymer Vesicles. All the polymer solutions were prepared in pure water, and the concentration of each polymer solution is 0.1 wt %. Then the aqueous solution of h-PAMAM was dropped into the aqueous solution of l-PAA under the mild stirring. The dosage of h-PAMAM or l-PAA solution was dependent on the complex ratio of h-PAMAM/l-PAA in the final mixing solution (see section 3.1.1). With addition of the h-PAMAM solution, the mixing solution gradually showed faint blue opalescence or white milk-like turbidity, indicated by the formation of the self-assembled aggregates of h-PAMAM/l-PAA. The final pHs of all mixed solutions were adjusted by adding hydrochloric acid (HCl; 1.0, 0.5, and 0.1 mol/L) or sodium hydroxide (NaOH; 1.0, 0.5, and 0.1 mol/L) aqueous solution.

2.4. Preparation of Complex Self-Assembled Fluorescent Polymer Vesicles. The fluorescent labeling of h-PAMAM was prepared as follows: 2.0 g of h-PAMAM was dissolved in 20 mL of deionized water. Then 10.0 mg of FITC was added into it, and the mixture was kept stirring at 30 °C for 60 h. The FITC labeled h-PAMAM were obtained by precipitating in acetone and drying in vacuum. The resulting FITC labeled h-PAMAM was purified by reprecipitation three times.

Three milliliters of the FITC labeled h-PAMAM aqueous solution (0.1 wt %) was mixed with 2 mL of the l-PAA aqueous solution (0.1 wt %). The pH of the mixed solution was adjusted to 5.0, and some self-assembled aggregates formed. The resulting aggregates were observed by laser confocal scanning microscopy (LCSM).

2.5. Preparation of the Stable Hollow Spheres. The hollow structure of the h-PAMAM/l-PAA vesicles can be stabilized by cross-linking the h-PAMAM layer as follows. On the basis of the mole number of primary amino groups in the h-PAMAM/l-PAA hollow spheres, 110 mol % of glutaric dialdehyde was added into the mixture and was kept stirring at room temperature overnight. Some precipitates appeared in this process and were collected by centrifugation. To remove the l-PAA ingredient, the precipitates were soaked in NaOH aqueous solution (2.0 mol/L) under mild stirring overnight, followed by centrifugation for three cycles. Then the precipitates were further washed by pure water to remove the residual NaOH and dried. The stable hollow spheres of cross-linked h-PAMAM were achieved.

2.6. Characterizations and Measurements. (1) ¹H nuclear magnetic resonance (NMR) and ¹³C NMR were tested on a MERCURY plus-400 spectrometer (Varian, Inc.) at 20 °C in DMSO-*d*₆. (2) Gel permeation chromatography (GPC) was carried out on a Perkin-Elmer Series 200 system at 70 °C (100 mL injection column, PL gel 10 μm 300 × 7.5 mm mixed-B columns, polystyrene calibration). DMF was used as the eluent, and the flow rate was 1.0 mL/min. (3) Fourier transform infrared (FTIR) spectra were recorded on an EQUINOX 55 spectrometer using a KBr window, and all the measurements were performed at ambient temperature. (4) Thermogravimetric analysis (TGA) was performed on a Perkin-Elmer apparatus with the heating rate of 20 °C/min under N₂ atmosphere. (5) Transmission electron microscopy (TEM) measurements were performed on a JEOL JEM-2100F transmission electron microscope at an accelerating voltage of 200 kV. The samples were prepared as follows: 5 μL of an aqueous solution of self-assembled aggregates was dropped onto a carbon-coated copper grid, then frozen, and dried by Freeze-Dryer ALPHA1-4 LDplus. The energy dispersing spectrum (EDS) analysis was obtained on the

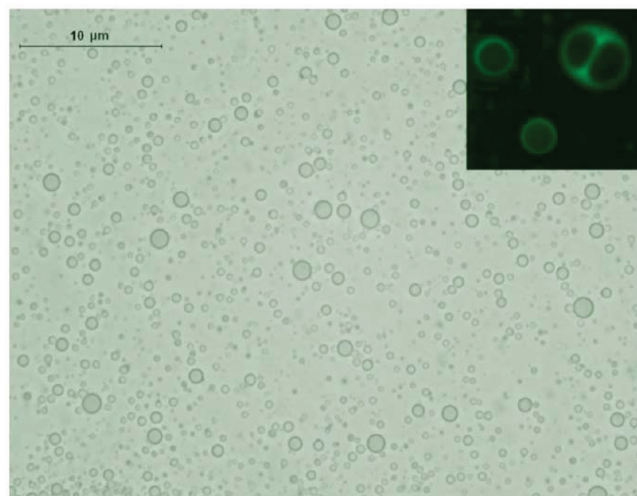


Figure 1. Micrograph image of the mixed h-PAMAM/l-PAA solution (pH = 5.0) after standing for one week. $R = 1.1:1$. Inset image: the confocal micrograph of the corresponding FITC labeled-h-PAMAM/l-PAA solution.

same TEM. (6) Atomic force microscopy (AFM) imaging was performed with the aid of a Nanoscope III-M system operating in tapping mode. The samples were prepared as follows: 5 μL of an aqueous solution of self-assembled aggregates was dropped onto freshly cleaved mica, then frozen, and dried by the same freeze-dryer. (7) For X-ray diffraction (XRD) analysis, the glass plates with samples were fixed on a sample holder and subjected to XRD analysis at room temperature on a D/MAX-2200/PC diffractometer. XRD patterns were recorded at a scanning rate of 4°/min in the 2θ range of 25–80° with Cu K α radiation ($\lambda = 1.541\ 78\ \text{Å}$). (8) Laser confocal scanning microscopy (LCSM) was performed on an AXIOPLAN 2 MOT laser confocal scanning microscope (ZEISS, Germany). (9) The transmittance of the solutions was measured on a GBC Cintra 10e UV–vis spectrophotometer (fixed wavelength 500 nm; slit width 1.5 nm). (10) Inductively coupled plasma-optical emission spectroscopy (ICP-OES) measurements were performed on a Prodigy instrument (Teledyne Leeman Laboratories Inc.). The samples were digested by chloronitrous acid for testing.

3. Results and Discussion

3.1. Morphology of the h-PAMAM/l-PAA Aggregates.

3.1.1. Effect of the Complex Ratio. Pure h-PAMAM or l-PAA is highly soluble in water. To our surprise, an interesting self-assembly phenomenon was observed in the process of mixing these two aqueous solutions. We further found the self-assembly process was affected by the complex ratio (named as R), which was defined as the molar ratio of amino groups in h-PAMAM to carboxyl groups in l-PAA. When the complex ratio R was in the range from 5:1 to 1:5, the resulting mixed solutions had faint blue opalescence. It indicates the self-assembled aggregates of h-PAMAM/l-PAA were formed. When R was close to 1:1 ($2:1 < R < 2:3$), the faint blue opalescence of the mixed solutions could be kept even if was stored for 1 week. However, some white precipitates were separated from the mixed solutions at the same condition when R was higher than 2:1 ($R > 2:1$) or lower than 2:3 ($R < 2:3$). Here the final pHs of all the mixed solutions were adjusted to 5.0.

The morphology of the self-assembled aggregates was observed preliminarily by optical and fluorescence microscopy. As can be seen in Figure 1, when R was equal to 1.1:1, a lot of spherical aggregates were found with a broad size distribution,

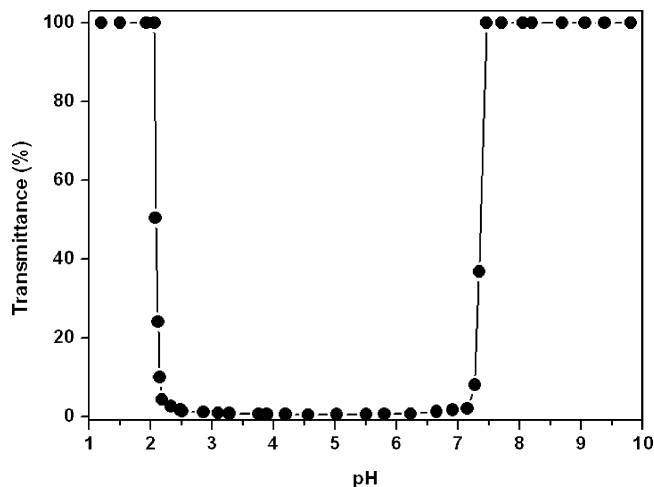


Figure 2. Transmittance of the h-PAMAM/I-PAA aqueous solution depended on its pH.

and most of them were in the range 1–2 μm . According to the fluorescent images of the corresponding self-assembled aggregates labeled FITC (insert image in Figure 1), their hollow structures were evidenced by the significant decrease of fluorescence intensity from the peripheral ring toward the center of the spheres.^{5c,8d,11} However, the self-assembled aggregates became unstable and even disappeared (see Supporting Information S1) when R was off 1:1 gradually. So we suppose that the strongest specific interactions could be formed when the R value was about 1 (i.e., at the equal mole of amino groups and carboxyl groups). Such interactions facilitate complexing of h-PAMAM with I-PAA in water and self-assembling into relatively stable vesicles.

3.1.2. Effect of the Solution pH. In experiments, we found that the complex self-assembly behavior at a certain R was also considerably affected by the final pH of the mixed solution. Here the stable mixed solutions of h-PAMAM/I-PAA ($R = 1$) with different pHs were selected and characterized by the spectrophotometer. The results in Figure 2 show that the transmittance of the mixed solution is a function of its pH. When the pH was lower than ca. 2.06 or higher than ca. 7.46, the mixed solution was kept transparent and its transmittance was almost close to 100%. When the pH was in the range of ca. 2.15–7.27, the mixed solution appeared totally cloudy and its transmittance nearly decreased to zero. It is clear that two abrupt jumps of turbidity appeared around pH 2.1 and pH 7.3.

TEM were further applied to investigate the morphologies of h-PAMAM/I-PAA aggregates at the different pHs, and the results are shown in Figure 3. At the basic pH (9.23), the aggregates were irregular spherical particles with the average diameter of 46 nm (Figure 3A) and the solution was transparent. When the pH was decreased to 7.16, the aggregates changed into vesicles with the average diameter of 157 nm (Figure 3B) and the solution became opaque with some light blue opalescence. When the pH was further decreased to 5.63, the average diameter of the vesicles even increased to 1400 nm, as shown in Figure 3C, and the solution became white and turbid. When the pH reached 2.16, the solution became opaque again with some light blue opalescence, and the average diameter of vesicles decreased to 369 nm. At the lower pH 2.08, the solution again became transparent, and the vesicles became smaller with the average diameter of 67 nm. Simultaneously, some of them changed into spherical particles, as shown in Figure 3E. When the pH was below 2.0, all the vesicles were changed into spherical particles again (Figure 3F).

On the basis of the above TEM results, it can be concluded that the average diameters of the h-PAMAM/I-PAA aggregates are quite dependent on the solution pH. The relationship curve between them is shown in Figure 4. It is clear that the diameters of the h-PAMAM/I-PAA aggregates experienced an increasing first and then decreasing process with decreasing the solution pH. Correspondingly, the h-PAMAM/I-PAA aggregates underwent a morphology transition from solid nanoparticles to vesicles and then back to solid nanoparticles. Therefore the above transmittance changes of the mixed solution were evidently attributed to such microstructural morphology changes of the h-PAMAM/I-PAA aggregates. It is noteworthy that the above transition process was reversible. More importantly, the h-PAMAM/I-PAA aggregates with the different morphologies and diameters could be obtained by adjusting the solution pH.

3.2. Explanation of the Complex Self-Assembly. **3.2.1. ζ Potentials.** The surface charges of the h-PAMAM/I-PAA aggregates depending on the solution pH were investigated by measuring the ζ potential of the mixed aqueous solution. As for the h-PAMAM/I-PAA aggregates in aqueous solution, their surface charges were changed from the positive to the negative with increasing the solution pH. The isoelectric point appeared at pH 4.6. This implicates that the outside surface and inner part of the h-PAMAM/I-PAA aggregates can be inverted by adjusting the solution pH. At the low solution pH, h-PAMAM was the outside surface of the aggregates. On the contrary, I-PAA became the outside surface of the aggregates at the high solution pH.

3.2.2. Mechanism of the Complex Self-Assembly. We propose that the complex self-assembly process is driven by the specific interactions between the carboxylic acid groups of I-PAA and the various amino groups of h-PAMAM. The morphology transition process is driven by the hydrophilic–hydrophobic balance depending on the solution pH.

When the solution pH was below ca. 2.1, the ionization of the carboxyl groups in I-PAA was greatly restrained. Thus, I-PAA chains were hydrophobic and tended to collapse together to avoid the unfavorable contact with water. However, the various amino groups in h-PAMAM were quaternized; thus h-PAMAM was very hydrophilic. At this condition, the complex process was probably performed between the collapsed I-PAA clusters and h-PAMAM molecules, which certainly resulted in the solid nanoparticles (Figure 6A) with I-PAA molecules forming the hydrophobic cores and the quaternized h-PAMAM molecules forming the hydrophilic shells.

With the increase of the solution pH from 2.2 to 7.5, the ionization degree gradually increased for I-PAA while it gradually decreased for h-PAMAM. According to ζ potential measurement, the isoelectric point was pH = 4.6 (Figure 5). When $2.2 < \text{pH} < 4.6$, the partially ionized I-PAAAs gained some hydrophilicity and were stretched in conformation. At this condition, the complex between I-PAA and h-PAMAM was probably performed at the molecular level. Since the partly ionized I-PAA was semirigid and its hydrophilicity was still smaller than that of the positively charged h-PAMAM molecules, the I-PAAAs tended to form the inner layer while h-PAMAMs tended to form outer shell to construct the bilayer structure.¹² As a result, polymer vesicles were generated (Figure 6B). Inversely, when $4.6 < \text{pH} < 7.5$, h-PAMAMs became semirigid and partly hydrophobic, while the hydrophilicity of the ionized I-PAA increased continuously. Thus, the molecular complex self-assembly resulted in the polymer vesicles with h-PAMAM inner layer and I-PAA outer shell (Figure 6C).

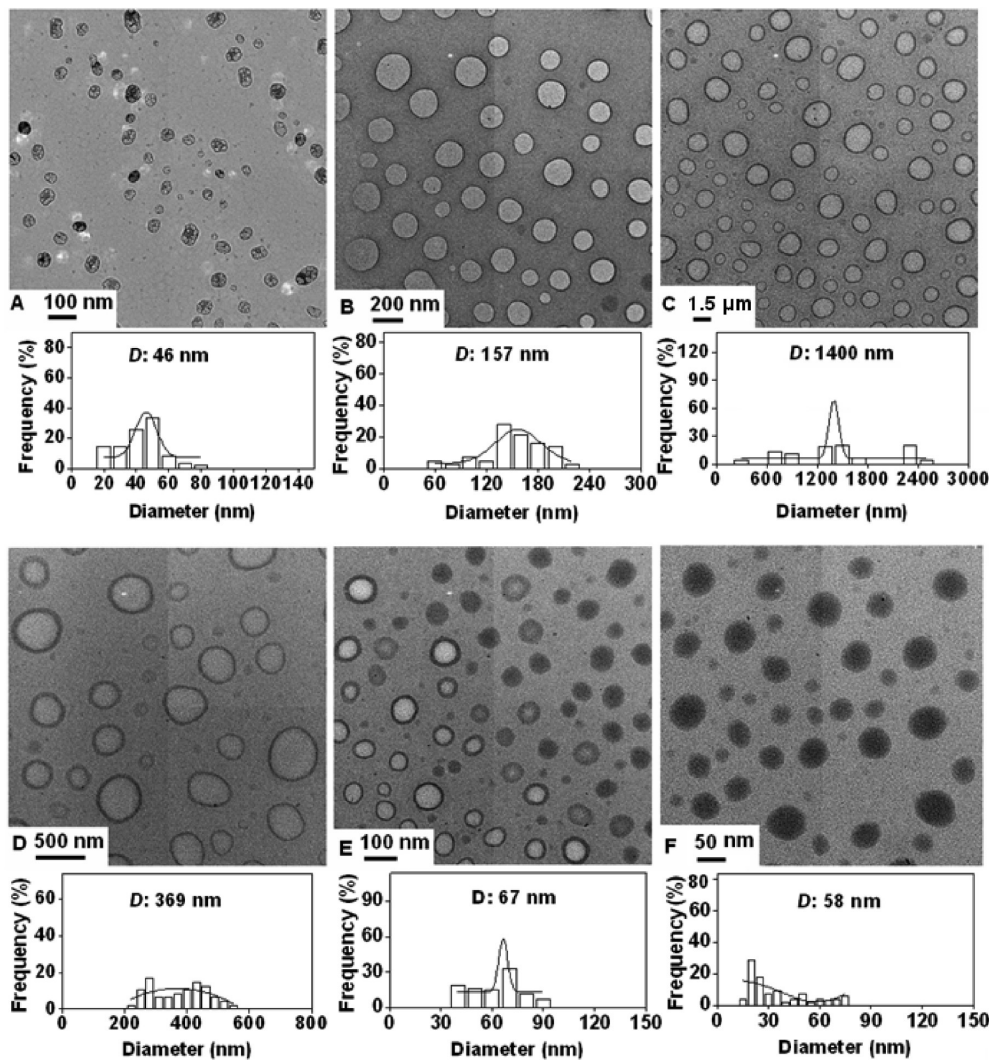


Figure 3. TEM images of h-PAMAM/l-PAA aggregates at the different pH and the corresponding size distribution histogram (the solid curve is a Gaussian fit to the data): (A) pH = 9.23; (B) pH = 7.16; (C) pH = 5.63; (D) pH = 2.16; (E) pH = 2.08; (F) pH = 1.78.

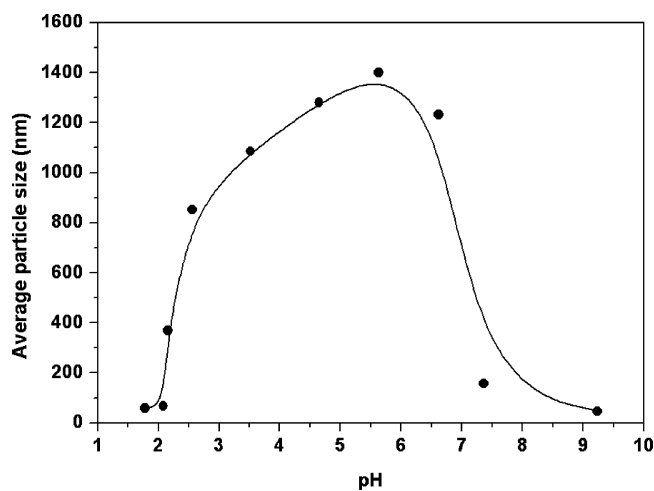


Figure 4. Relationship between the average diameters of the h-PAMAM/l-PAA aggregates and the solution pH.

When pH > 7.5, l-PAA was fully ionized and became very hydrophilic while h-PAMAMs were completely deprotonated and became hydrophobic. Thus, h-PAMAMs were quickly collapsed together to form clusters. The complex self-assembly of h-PAMAMs clusters and fully ionized l-PAA was performed to construct core-shell spherical aggregates (Figure 6D) with

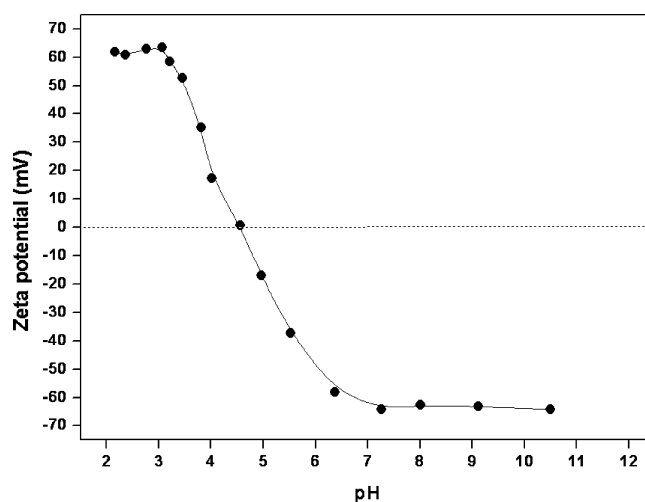


Figure 5. Relationship of the ζ potential and the solution pH of self-assembled h-PAMAM/l-PAA aggregates.

the collapsed hydrophobic h-PAMAM cores and the hydrophilic l-PAA shells.

3.3. Functionalization of the Self-Assembled Hollow Spheres.
3.3.1. Fixation of the Self-Assembled Hollow Spheres. It was found that the as-prepared hollow spheres by the complex self-assembly were sensitive to environmental impacts, such as

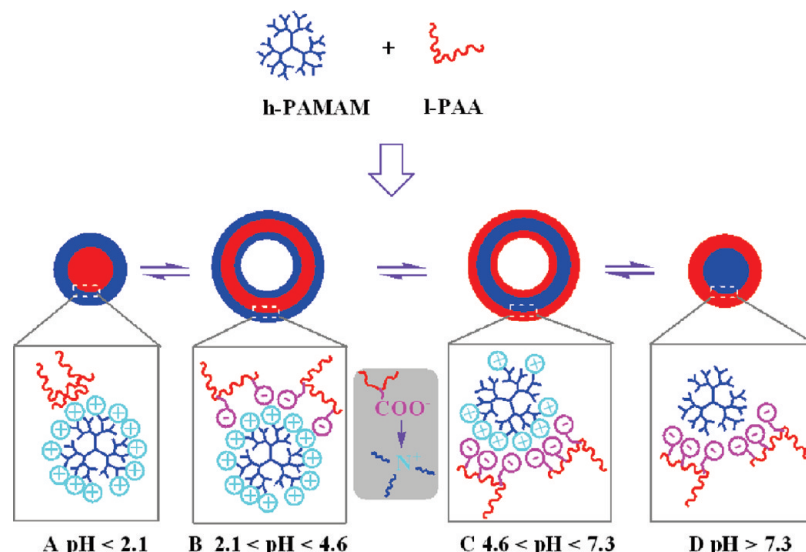


Figure 6. Plots for the complex self-assembly mechanism of h-PAMAM and I-PAA.

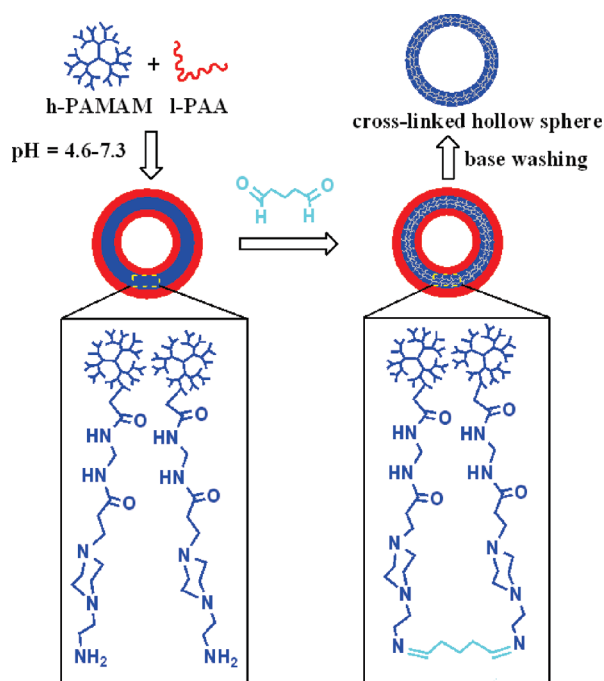


Figure 7. Chemical cross-linking of h-PAMAM/I-PAA vesicles.

solvent, pH, and temperature. For further applications, we tried to fix their hollow structures by chemical modifications. Around the neutral pH, some nonionized terminal primary amino groups in h-PAMAM could be cross-linked by GDA. The schematic illustration of this fixation process was shown in Figure 7. Typically, GDA (110 mol % in feed) was added into the aqueous solution of h-PAMAM/I-PAA at pH 4.6–7.3. The mixture was kept stirring at room temperature overnight. After centrifugation, the precipitates were collected and washed by NaOH aqueous solution (1.0 mol/L), deionized water, and alcohol in turn to remove the I-PAA layer. Some cross-linked h-PAMAM hollow spheres were obtained after being dried.

The cross-linked hollow structure of the resulting h-PAMAM spheres was confirmed by FTIR, optical microscopy, and TEM measurements. The FTIR spectrum of pure h-PAMAM displayed the absorption bands of amide I, amide II, and NH stretching at 1649, 1536, and 3268 cm^{-1} , respectively. However, these bands shifted to 1608, 1608, and 3430 cm^{-1} correspond-

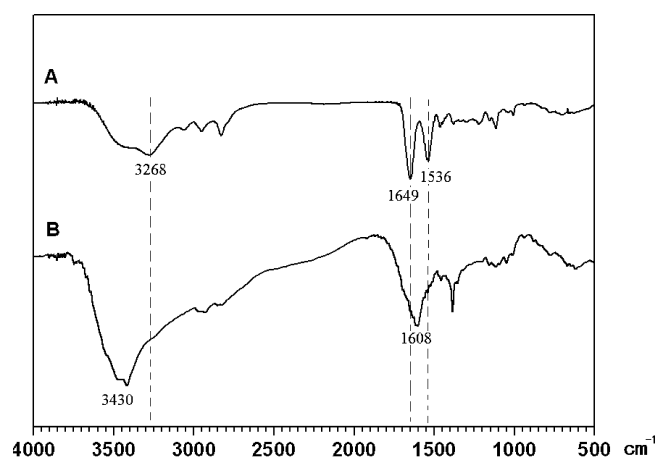


Figure 8. FTIR spectra of (A) pure h-PAMAM and (B) cross-linked h-PAMAM hollow spheres.

ingly in the cross-linked product (Figure 8). When the cross-linked aggregates were soaked in ethanol again, their hollow sphere structure was still kept and observed by the optical microscopy (Figure 9A–C). However, the un-cross-linked aggregates in water were dissociated when the ethanol was added. Moreover, the vesicles were broken up when the water was evaporated (Figure 9D). These results indicate that the hollow structure of the complex self-assembly aggregate was fixed successfully by the cross-linking reaction.

From the insert TEM images in Figure 9, numerous folds can be found on the cross-linked aggregates in the dry state. This is the typical characteristic of the polymeric hollow spheres. The outermost dark shell with the thickness of 60 nm was attributed to the cross-linked h-PAMAM layer. The obvious difference between the inner part and the outermost part of the aggregates could be attributed to their hollow structures. The diameter of the aggregates was in the range from 0.5 to 2 μm . Besides the folding hollow spheres, some irregular mottles can also be observed. It indicated that partial self-assembled h-PAMAM aggregates were broken due to the stirring in the period of cross-linking reaction.

3.3.2. Carriers for Noble Metals. The application of the hollow spheres based on polymers has become a hot topic, as mentioned above. They can be widely used as drug or catalyst carriers.^{2,13} Here our cross-linked hollow spheres of h-PAMAM

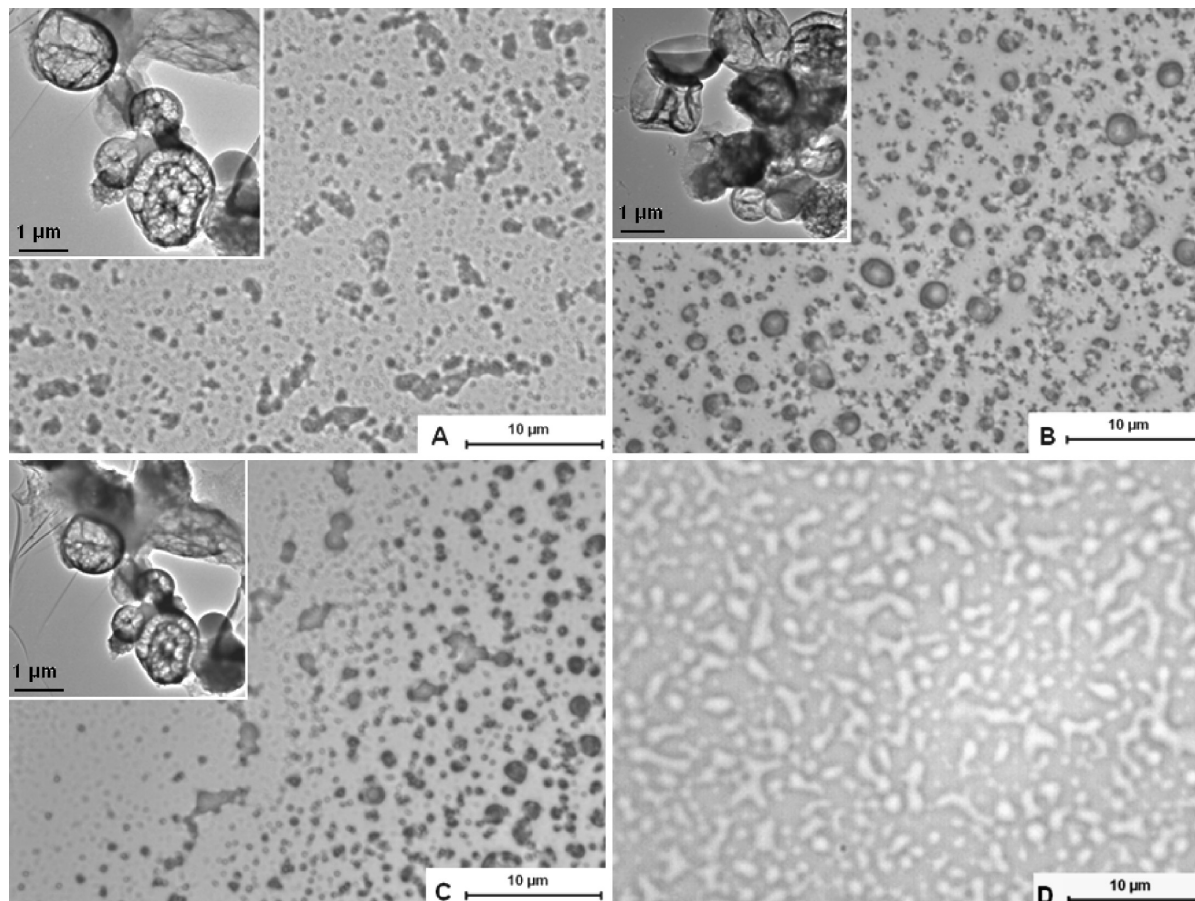


Figure 9. Optical microscopy images of the cross-linked aggregates soaked in ethanol, prepared from the self-assembled vesicles at the pH of (A) 5.2, (B) 6.5, and (C) 7.5. (D) Un-cross-linked aggregates at the pH of 6.5 after the water evaporated. Inset: corresponding TEM images.

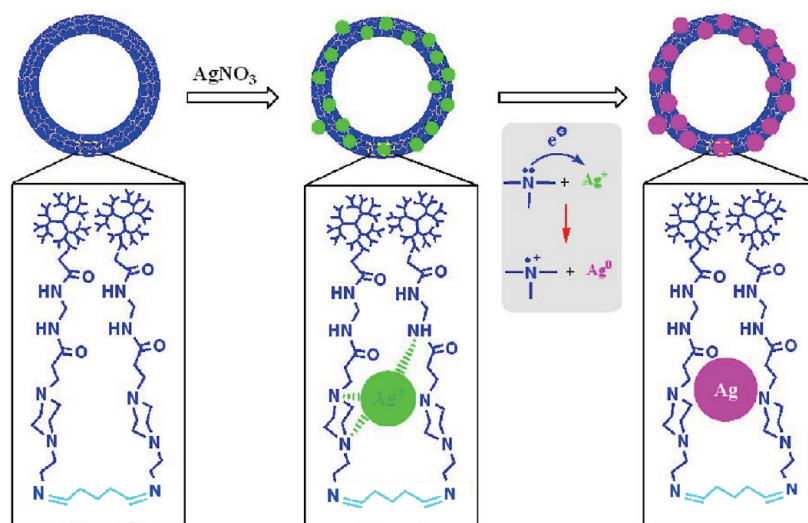


Figure 10. Cross-linked hollow spheres of h-PAMAM to load silver.

could be also used as the carriers. Other than previous reports, interestingly, our cross-linked hollow spheres could absorb the different metal cation from water, reduced them into corresponding nanoparticles in situ and produced the polymer/metal (Ag, Au, or Pd) hybrid spheres at last.

The schematic process for the preparation of the hybrid spheres containing silver was shown in Figure 10. When the AgNO_3 aqueous solution was added into the aqueous dispersion of the cross-linked hollow spheres, the amino groups in the cross-linked h-PAMAM layer were coordinated with Ag^+ s

effectively. Then the single electron transfer occurred and the Ag^+ s were reduced in situ into Ag nanoparticles. In this process, the cross-linked h-PAMAM layer acted as both the stabilizing and reducing agent.^{10,14} Such an approach for loading metallic nanoparticles was rather convenient and straightforward without any extra reductant.

The TEM images in Figure 11 showed that various nanoparticles (Au, Ag, or Pd) were loaded effectively into the h-PAMAM shell of the cross-linked hollow spheres. The Pd or Au nanoparticles with about 10 nm diameters dispersed well in

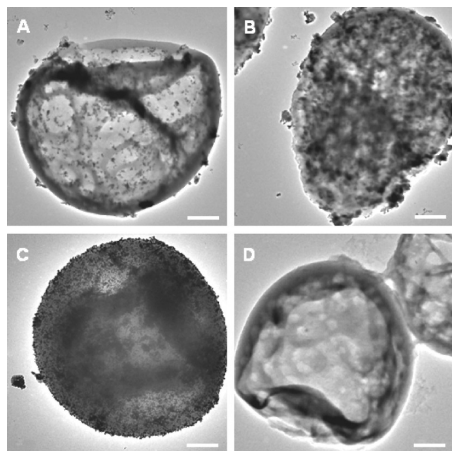


Figure 11. TEM images of the cross-linked hollow spheres of h-PAMAM (A) loading Au, (B) loading Ag, (C) loading Pd, and (D) loading nothing. Scale bars are 500 nm.

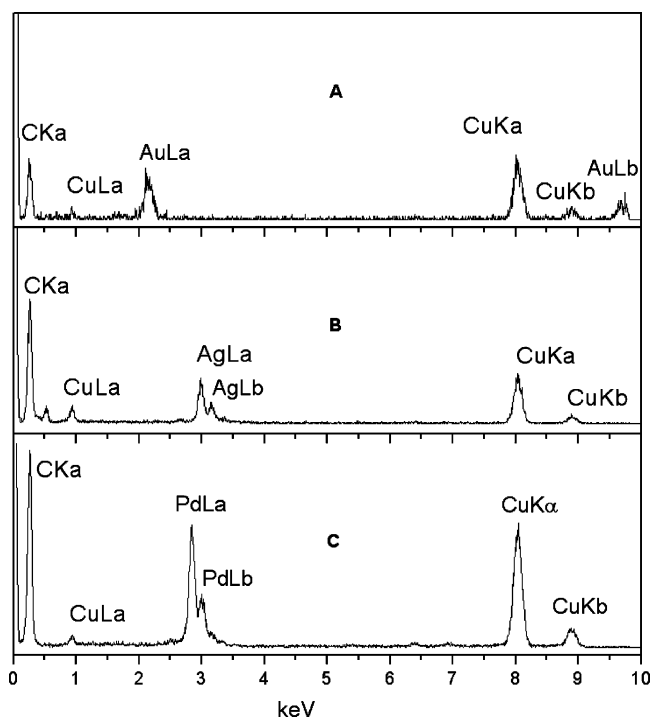


Figure 12. EDS spectra of the cross-linked hollow spheres of h-PAMAM (A) loading Au, (B) loading Ag, and (C) loading Pd.

the spheres. But for the Ag nanoparticles, some agglomeration of them was found in the spheres. The morphology difference of various metal nanoparticles may be correlative to the formation and growth of their crystal nucleus. Besides, the cross-linked hollow spheres of h-PAMAM may also have some inductive effects on the crystal growing.¹⁵ The EDS measurement further confirmed the successful carrying of Au, Ag, or Pd nanoparticles in the cross-linked hollow spheres of h-PAMAM and the corresponding spectra were shown in Figure 12. The loading capacity of the resulting cross-linked hollow spheres for various noble metals was ca. 15.5 wt % for Au, 12.0 wt % for Ag, and 8.2 wt % for Pd, respectively, by EDS measurement (15.2 wt % for Au, 12.3 wt % for Ag, and 8.0 wt % for Pd, respectively, by TGA data in Supporting Information S3; 15.7 wt % for Au, 11.8 wt % for Ag, and 8.4 wt % for Pd, respectively, by ICP-OES measurements).

4. Conclusion

In conclusion, a novel kind of polymeric hollow spheres was prepared successfully by the complex self-assembly of h-PAMAM/l-PAA in aqueous solution. The morphology transition of the self-assembled aggregates from solid particles to vesicles could be realized by adjusting the solution pH. When the solution pH was lower than 2.1, the assembled aggregates were solid nanoparticles with l-PAA as the core and the protonated h-PAMAM as the shell. On the contrary, when the solution pH was larger than 7.5, the resulting solid nanoparticles consisted of the h-PAMAM core and the solvated l-PAA shell. When the solution pH was in the range from 2.1 to 7.3, the aggregates became vesicles with typical hollow structures. Interestingly, the inverting of the inner surface and outer surface occurred in the vesicle when the solution pH equals 4.6. The driving forces of the complex self-assembly can be ascribed to the hydrophilic–hydrophobic balance and the specific interactions between the carboxylic acid groups in l-PAA and various amino groups in h-PAMAM. The hollow structure of the self-assembled vesicles can be stabilized by using GDA to cross-link the h-PAMAM layer. The resulting cross-linked hollow spheres can encapsulate various noble metallic cations and reduce them into nanoparticles *in situ*. The loading capacity of them for various noble metals was ca. 15.5 wt % for Au, 12.0 wt % for Ag, and 8.2 wt % for Pd, respectively. Such hybrid materials can be potentially applied in metal catalysis.

Acknowledgment. We gratefully acknowledge financial support provided by the National Basic Research Program (2007CB808000), National Natural Science Foundation of China (No. 50873058, No.50633010, No. 50503012), and Shanghai Leading Academic Discipline Project (No. B202).

Supporting Information Available: Optical microscopy images of the self-assembled aggregates, TEM images of the vesicles at the different solution pH, and the TGA curves of the different cross-linked hollow spheres of h-PAMAM, and AFM images of the hollow spheres before and after crosslinking. This material is available free of charge via the Internet at <http://pubs.acs.org>.

References and Notes

- (1) (a) Muthukumar, M.; Ober, C. K.; Thomas, E. L. *Science* **1997**, *277*, 1225. (b) Stupp, S. I.; LeBonheur, V.; Walker, K.; Li, L. S.; Huggins, K. E.; Keser, M.; Amstutz, A. *Science* **1997**, *276*, 384. (c) Caruso, F.; Caruso, R. A.; Mohwald, H. *Science* **1998**, *282*, 1111. (d) Klok, H. A.; Lecommandoux, S. *Adv. Mater.* **2001**, *13*, 1217. (e) Dennis, E. D.; Eisenberg, A. *Science* **2002**, *297*, 967. (f) Bergbreiter, D. E. *Angew. Chem., Int. Ed.* **1999**, *38*, 2870. (g) Liu, X. K.; Jiang, M. *Angew. Chem., Int. Ed.* **2006**, *45*, 3846. (h) Lattuada, M.; Hatton, T. A. *J. Am. Chem. Soc.* **2007**, *129*, 12878. (i) Vanhest, J. C. M.; Delnoye, D. A. P.; Baars, M. W. P. L.; Van Genderen, M. H. P.; Meijer, E. W. *Science* **1995**, *268*, 1592. (j) Ariga, K.; Hill, J. P.; Lee, M. V.; Vinu, A.; Charvet, R.; Acharya, S. *Sci. Technol. Adv. Mater.* **2008**, *9*, 014109. (k) Zhou, Y. F.; Yan, D. Y. *Chem. Commun.* **2009**, *10*, 1172.
- (2) (a) Liu, S. Y.; Billingham, N. C.; Armes, S. P. *Angew. Chem., Int. Ed.* **2001**, *40*, 2328. (b) Gohy, J.; Antoun, S.; Jerome, R. *Macromolecules* **2001**, *34*, 7435. (c) Mao, Z. W.; Ma, L.; Gao, C. Y.; Shen, J. C. *J. Controlled Release* **2005**, *104*, 193. (d) Ahmed, F.; Pakunlu, R. I.; Srinivas, G.; Brannan, A.; Bates, F.; Klein, M. L.; Minko, T.; Discher, D. E. *Mol. Pharm.* **2006**, *3*, 340. (e) Ilhan, F.; Galow, T. H.; Gray, M.; Clavier, G.; Rotello, V. M. *J. Am. Chem. Soc.* **2000**, *122*, 5895.
- (3) (a) Kabanov, A. V.; Bronich, T. K.; Kabanov, V. A.; Yu, K.; Eisenberg, A. *J. Am. Chem. Soc.* **1998**, *120*, 9941. (b) Butun, V.; Armes, S. P.; Billingham, N. C. *Macromolecules* **2001**, *34*, 1148. (c) Tsuda, K.; Dol, G. C.; Gensch, T.; Hofkens, J.; Latterini, L.; Weener, J. W.; Meijer, E. W.; de Schryver, F. C. *J. Am. Chem. Soc.* **2000**, *122*, 3445. (d) Won, Y.-Y.; Brannan, A. K.; Davis, H. T.; Bates, F. S. *J. Phys. Chem. B* **2002**, *106*, 3354. (e) Du, J.; Tang, Y.; Lewis, A. L.; Armes, S. P. *J. Am. Chem. Soc.* **2005**, *127*, 17982. (f) Wu, J.; Eisenberg, A. *J. Am. Chem. Soc.* **2006**,

128, 2880. (g) Liu, X. Y.; Wu, J.; Kim, J.-S.; Eisenberg, A. *Langmuir* **2006**, *22*, 419. (h) Dai, C.-A.; Yen, W.-C.; Lee, Y.-H.; Ho, C.-C.; Su, W.-F. *J. Am. Chem. Soc.* **2007**, *129*, 11036.

(4) (a) Donath, E.; Sukhorukov, G. B.; Caruso, F.; Davis, S. *Angew. Chem. Int. Ed.* **1998**, *37*, 2202. (b) Jenekhe, S. A.; Chen, X. L. *Science* **1999**, *283*, 372. (c) Bronich, T. K.; Ouyang, M.; Kabanov, V. A.; Eisenberg, A.; Szoka, F. C., Jr.; Kabanov, A. V. *J. Am. Chem. Soc.* **2002**, *124*, 11872. (d) Breiteukamp, K.; Emrick, T. *J. Am. Chem. Soc.* **2003**, *125*, 12070. (e) Jungmann, W.; Schmidt, M.; Ebenhoch, J.; Weis, J.; Maskos, M. *Angew. Chem., Int. Ed.* **2003**, *42*, 1714. (f) Beil, J. B.; Zimmerman, S. C. *Macromolecules* **2004**, *37*, 778.

(5) (a) Kuang, M.; Duan, H.; Wang, J.; Jiang, M. *J. Phys. Chem. B* **2004**, *108*, 16023. (b) Luo, L. B.; Eisenberg, A. *Angew. Chem., Int. Ed.* **2002**, *41*, 1001. (c) Thibault, R. J., Jr.; Galow, T. H.; Turnberg, E. J.; Gray, M.; Hotchkiss, P. J.; Rotello, V. M. *J. Am. Chem. Soc.* **2002**, *124*, 15249. (d) Liu, F. T.; Eisenberg, A. *J. Am. Chem. Soc.* **2003**, *125*, 15059.

(6) (a) Rodriguez-Hernandez, J.; Babin, J.; Zappone, B.; Lecommandoux, S. *Biomacromolecules* **2005**, *6*, 2213. (b) Li, Y.; Lokitz, B. S.; McCormick, C. L. *Angew. Chem., Int. Ed.* **2006**, *45*, 5792.

(7) (a) Gao, C.; Yan, D. Y. *Prog. Polym. Sci.* **2004**, *29*, 183. (b) Yan, D. Y.; Zhou, Y. F.; Hou, J. *Science* **2004**, *303*, 65. (c) Zhang, Y. W.; Huang, W.; Zhou, Y. F.; Yan, D. Y. *Chem. Commun.* **2007**, 2587. (d) Ornatka, M.; Peleshanko, S.; Genson, K. L.; Rybak, B.; Bergman, K. N.; Tsukruk, V. V. *J. Am. Chem. Soc.* **2004**, *126*, 9675.

(8) (a) Zhou, Y. F.; Yan, D. Y. *Angew. Chem., Int. Ed.* **2004**, *43*, 4896. (b) Zhou, Y. F.; Yan, D. Y. *Angew. Chem., Int. Ed.* **2005**, *44*, 3223. (c) Zhou, Y.; Yan, D.; Dong, W.; Tian, Y. *J. Phys. Chem. B* **2007**,

111, 1262. (d) Mai, Y. Y.; Zhou, Y. F.; Yan, D. Y. *Small* **2007**, *3*, 1170. (e) Mai, Y. Y.; Zhou, Y. F.; Yan, D. Y. *Macromolecules* **2005**, *38*, 8679.

(9) Zhang, Y. W.; Huang, W.; Zhou, Y. F.; Yan, D. Y. *Chem. Commun.* **2007**, 2587.

(10) Zhang, Y. W.; Peng, H. S.; Huang, W.; Zhou, Y. F.; Zhang, X. H.; Yan, D. Y. *J. Phys. Chem. C* **2008**, *112*, 2330.

(11) Meng, F.; Hiemstra, C.; Engbers, G. H. M.; Feijen, J. *Macromolecules* **2003**, *36*, 3004.

(12) (a) Schenning, A. P. H. J.; Elissen-Roman, C.; Weener, J. W.; Baars, M. W. P. L.; van der Gaast, S. J.; Meijer, E. W. *J. Am. Chem. Soc.* **1998**, *120*, 8199. (b) Antonietti, M.; Forster, S. *Adv. Mater.* **2003**, *15*, 1323.

(13) Mangeney, C.; Bousalem, S.; Connan, C.; Vaulay, M.-J.; Bernard, S.; Chehimi, M. M. *Langmuir* **2006**, *22*, 10163.

(14) (a) Kuo, P. L.; Chen, C.-C.; Jao, M.-W. *J. Phys. Chem. B* **2005**, *109*, 9445. (b) Chen, C.-C.; Hsu, C.-H.; Kuo, P.-L. *Langmuir* **2007**, *23*, 6801. (c) Lazareva, N. F.; Vakul'skaya, T. I.; Albanov, A. I.; Pestunovich, V. A. *Appl. Organomet. Chem.* **2006**, *20*, 696. (d) Zhou, Y.; Itoh, H.; Uemura, T.; Naka, K.; Chujo, Y. *Langmuir* **2002**, *18*, 277. (e) Keki, S.; Torok, J.; Deak, G.; Daroczi, L.; Zsuga, M. *J. Colloid Interface Sci.* **2000**, *229*, 550.

(15) (a) Matrices, R. S.; Breen, C. A.; Solis, D. J.; Swager, T. M. *Chem. Mater.* **2006**, *18*, 21. (b) Manna, S.; Batabyal, S. K.; Nandi, A. K. *J. Phys. Chem. B* **2006**, *110*, 12318. (c) Perkin, K. K.; Turner, J. L.; Wooley, K. L.; Mann, S. *Nano Lett.* **2005**, *5*, 1457.

JP810221B